

Seismic vulnerability assessment of a typical 3 span highway bridge in Bangladesh

Md. Rashedul Kabir

Department of Civil Engineering, Ahsanullah University of Science & Technology, Dhaka-1208, Bangladesh

A.H.M. Muntasir Billah & M. Shahria Alam

School of Engineering, University of British Columbia, Kelowna, BC, Canada

ABSTRACT: Seismic vulnerability of a three span continuous highway bridge located in Kishoreganj, Bangladesh is assessed numerically in this study. Fragility function, which expresses the likelihood of exceeding a damage state conditioned at a given earthquake intensity, has been derived based on nonlinear incremental dynamic analysis results of the bridge subjected to medium to strong earthquake excitation records. A total of 20 excitation records with peak ground acceleration values ranging from 0.37 to 1.07 g, are used in the nonlinear dynamic analysis of the bridge. A 2-D finite element model scheme is used in this study considering nonlinearity in the bridge piers and the isolation bearings. The fragility curves are constructed for two bridge components (i.e. piers and isolation bearings), and the system as well. The component fragility curves are then combined to evaluate the fragility curves for the entire bridge system at different damage states. The numerical results show that the failure probability of the bridge system is dominated by the bridge piers over the isolation bearings.

1 INTRODUCTION

For a sustainable and effective transportation system, we need to look beyond roads where the essentiality of highway bridges cannot be overlooked. Every year a great deal of money is spent worldwide to fix the bridges in need of repair and to construct new ones. The performance of highway bridge systems observed in past and recent earthquakes- including the 1971 San Fernando earthquake, the 1994 Northridge earthquake, the 1995 Great Hanshin earthquake in Japan, the 1999 Chi-Chi earthquake in Taiwan, the 2010 Chile earthquake, and the 2010 Haiti earthquake have demonstrated that bridges are highly susceptible to damages during earthquakes (Basöz et al. 1999). The highway bridges in Bangladesh are no exception to that. Bangladesh is located in a tectonically active area. It sits where three tectonic plates meet: the Indian Plate, the Eurasian Plate, and the Burmese Plate. The meteorological department of Bangladesh University of Engineering and Technology (BUET) detected at least 90 earthquakes taking place in the country between May 2007 and July 2008, nine of them above five on the Richter scale and epicentres of 95 percent being within a 600 km radius of Dhaka city (Ferdousi & Rahman 2010). These minor tremors clearly indicate the possibility of more powerful earthquakes striking the country. In total, there are 4,659 numbers of bridges in Bangladesh and only the major bridges cover about 21 km of the transportation network (<http://www.rhd.gov.bd/>). Vulnerability assessment of these huge numbers of highway bridges is in demand to get prepared and take precautions required to fight accidental tremor.

Since highway bridges are critical components in a transportation network system, it is important to perform their seismic vulnerability assessment and such assessment is widely accepted as a useful technique for the prioritization of seismic retrofitting, disaster response planning, estimation of direct monetary loss, and evaluation of loss of functionality of highway systems in the event of an earthquake. Seismic vulnerability of highway bridges is usually expressed in the form of fragility functions, which display the conditional probability of structural demand (structural response) caused by various levels of ground shaking that exceed the structural capacity defined by a damage state (Hwang et al. 2001). After recognizing the usefulness of bridge vulnerability information in assessing, managing, and reducing seismic risk, different fragility-curve generation methodologies have been developed, involving probabilistic seismic performance evaluation of highway bridges. Some of these methodologies are based on expert opinion (ATC 1985), some are empirically formulated based on observed damage from past earthquakes (Basöz et al. 1999, Shinozuka et al. 2000), while others are derived from analytical simulation methods (Choi et al. 2004, Hwang et al. 2000, 2001, Mackie & Stojadinović 2004, Nielson 2005, Nielson & DesRoches 2007a, b, Bhuiyan & Alam 2012). Details of different methods of fragility as-

assessment can be found in Billah & Alam (2014a). Though all of the methodologies have their own limitations in evaluating the probabilistic seismic performance of highway bridges, fragility assessment methodologies using analytical approaches have been widely adopted since they are more readily applicable to bridge types and geographical regions where seismic bridge damage records are insufficient. Considering the damage database of Bangladesh, the analytical approach seems to be the appropriate one for the fragility assessment of highway bridges.

To improve the seismic performance and subsequently reduce the seismic vulnerability of both new and existing bridges, different forms of seismic isolation devices have been commonly employed in the last few decades (Buckle & Mayes 1990, Dezfuli & Alam 2013). Due to their flexibility, isolation devices can increase the natural period of the bridge to evade the dominant frequency of earthquake ground motions. In addition, the inherently occupied damping property and energy dissipation mechanism prevents the bridge system from over displacement (Kelly 1997).

The objective of this paper is to evaluate the seismic vulnerability of an isolated bridge in both the longitudinal and transverse directions with elastomeric rubber bearing as isolation devices. In this regard, a three-span continuous highway bridge of 75.38 m length named Sharifpur Bridge located in Kishoreganj, Bangladesh is considered as the physical model to analyze. The analytical simulation method based on nonlinear incremental dynamic analysis (IDA) is used in evaluating the seismic fragility functions of the bridge using 20 ground motion records. A two-dimensional (2-D) finite-element model scheme with nonlinear force-displacement relationships for the bridge piers and the isolation bearings are used in the analytical modelling of the bridge. A total of 20 excitations with peak ground accelerations (PGA) ranging from 0.37 g to 1.07 g having different ground conditions are considered in the IDA of the bridge. Only two bridge components, isolation bearings and bridge piers, are considered in generating the seismic fragility functions for the bridge at different damage states. These component fragilities are then joined together to obtain an estimate of the overall fragility function of the bridge system.

2 BRIDGE CHARACTERISTICS

A three-span continuous highway bridge isolated by elastomeric rubber bearing is considered in this study, as shown in Figures 1a, b, c. The bridge consists of reinforced concrete (RC) deck-girder system isolated by rubber bearings installed below the concrete girder supported on top of RC pier cap (Fig. 1a). The superstructure consists of 200 mm RC slab covered by 75 mm of asphalt layer shown in Figure 1c. The height of the continuous concrete girder is 1,325 mm (Fig. 1c). The substructures consist of RC piers and footings supported on deep pile foundation. The reinforcement details of the bridge pier consist of 30- D32 (diameter 32 mm) longitudinal reinforcements with 12 mm diameter spiral at 75 mm pitch. In the longer direction of pier cap, 24-D25 (diameter 25 mm) rebars are distributed on top in two layers and 20-D25 (diameter 25 mm) rebars at the bottom. Four D16 (diameter 26 mm) rebar is used as face bar. 4 leg 12mm stirrup spaced 150 mm c/c (centre to centre) are provided as shear reinforcements. Piers are supported by 13 cast-in-situ concrete piles connected by pile a cap. Length of the piles is 24 m with 750 mm diameter (shown in Fig. 1b). Piles below abutments are identical with 20 in numbers. The geometric details and material properties of the bridge deck and piers with footings are presented in Table 1. The geometry and material properties of rubber bearings are presented in Table 2.

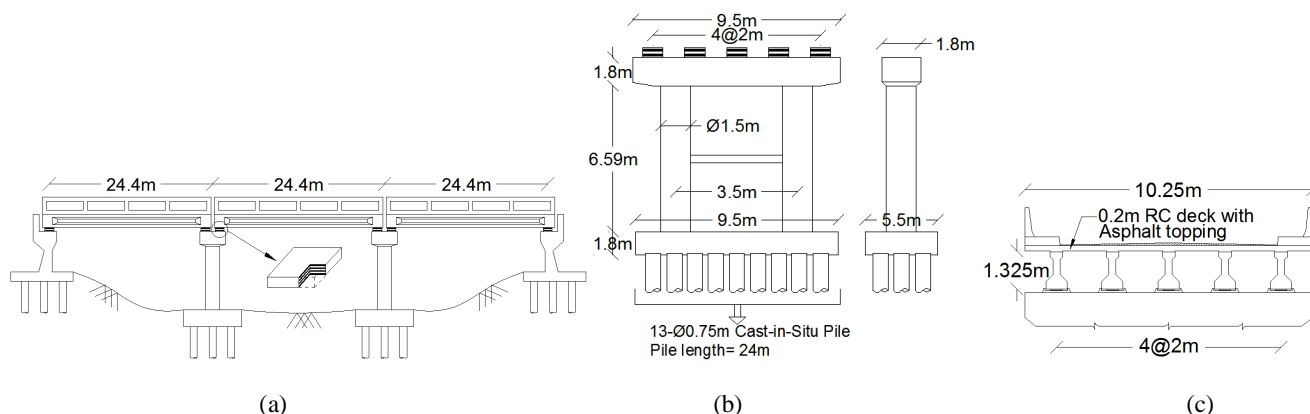


Figure 1. Geometric details of the bridge (a) longitudinal view and general elevation (b) transverse and longitudinal view of the bridge pier (c) transverse section of the superstructure; all dimensions are in m.

Table 1. Geometries and material properties of the bridge.

Properties	Specifications
Cross section of the pier cap (mm ²)	1,800 x 9,500
Diameter of pier (mm)	1,500
Height of the pier (mm)	6,590
Cross section of the pile cap (mm ²)	5,500 x 10,500
Diameter of pile (mm)	750
Length of pile (m)	24
No. of pile below piers	13
28 Days concrete strength (MPa)	20
Unit weight of concrete (kN/m ³)	24
Young's modulus of elasticity of steel (MPa)	200,000
Yield strength of steel (MPa)	413

Table 2. Geometries and material properties of isolation bearings

Properties	Specifications
Cross section of the bearing (mm ²)	400 x 500
Thickness of rubber layer (mm)	17
Number of rubber layers	3
Thickness of steel layer (mm)	3
Number of steel layers	4
Allround rubber envelope thickness (mm)	5

3 ANALYTICAL MODELING OF THE BRIDGE

The entire longitudinally straight multi-span continuous highway bridge system is approximated as a continuous 2-D finite element frame using the nonlinear analysis program SeismoStruct (SeismoStruct 2014). Analytical model of the bridge pier with girder is shown in Figure 2a. The sufficiency of 2-D model approach when the bridge is longitudinally straight has been proven by the works of Choi et al. (2004), Zhang & Huo (2009). Although the current analysis has been performed using a freely available software, the exactness and accuracy of the programme is verified by several experimental results that consist of static and dynamic loading of structures (Alam et al. 2008, Billah & Alam 2012). A finite element model with frame and spring elements is used to approximate the continuous system of the bridge with a finite number of degrees of freedom. The superstructure and substructure of the bridge are modeled as a lumped mass system divided into a number of small discrete segments. The mass of each segment is assumed to be distributed between the two adjacent nodes in the form of point mass. The details of modeling of a typical bridge pier along with deck are given in Figure 2b.

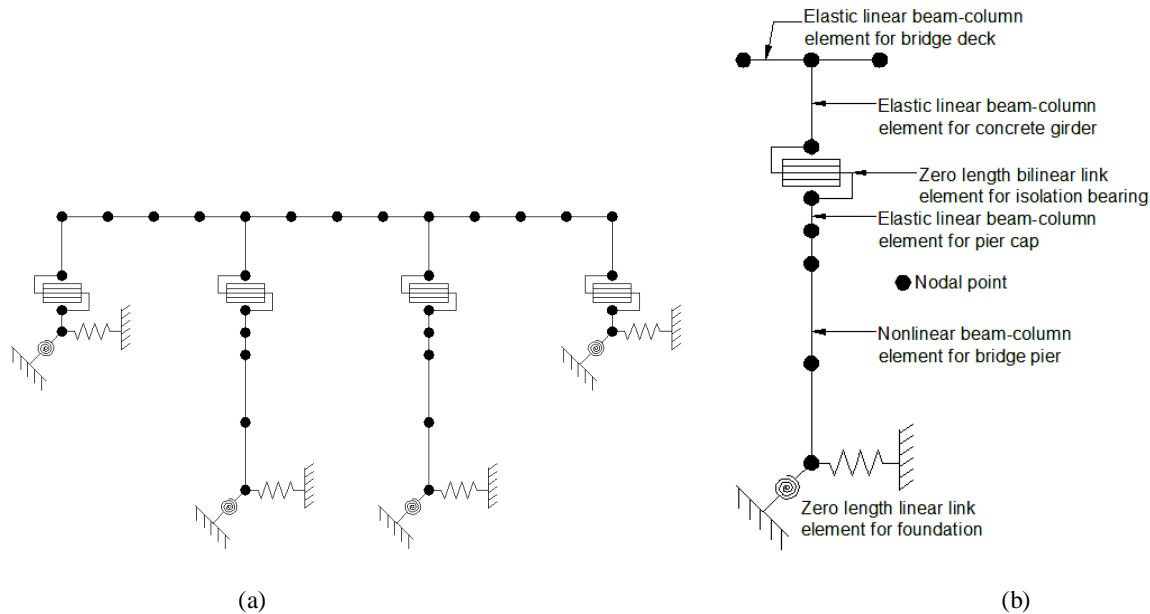


Figure 2. Analytical model of the bridge system (a) 2-D finite element model of the bridge system including nonlinear model used for isolation bearings and bridge pier, and (b) details of modeling of an internal bridge pier.

The superstructure consisting of RC bridge deck and concrete I-girders is modeled using linear beam-column elements so that the superstructure remains elastic under the seismic loads. The stiffness of the superstructure does not have a significant effect on the seismic response of the bridge (Ghobarah & Ali 1988) since the response is typically governed by the isolation bearings, bridge piers, and foundation (Choi et al. 2004). The nonlinear force-displacement behavior of the bridge pier is considered in this seismic analysis. The bridge piers are modeled using the fiber elements. Each fiber has a stress-strain relationship, which can be specified to represent unconfined concrete, confined concrete, and longitudinal steel reinforcement. The confinement effect of the concrete section is considered on the basis of reinforcement detailing.

The footing-foundation movement is modeled using linear translational and rotational springs. Medium dense to very dense sandy soil property is considered in modeling the footing spring and damping characteris-

tics. The pile model used in computing the spring stiffness and damping parameters in both the translational and longitudinal direction is employed following the model developed by Novak (1974), Prakash & Sharma (1990). The stiffness and damping contribution due to side friction of the pile cap are adopted from Novak (1974), Prakash & Puri (1988). Stiffness and damping parameters of horizontal response for piles is taken from Novak and Sharnouby (1983). Group effect (Poulos 1971) and torsional vibrations (Novak & Howell 1977) of piles are also considered in the modeling phase. In the abutment model, an additional passive soil contribution in the longitudinal direction is considered (Caltrans 1990, 2006).

The subject structure is isolated by elastomeric rubber bearing which is widely used all over the world due to their high damping properties. The behavior of the elastomeric pad is characterized by sliding. This sliding behavior is characterized by the initial stiffness which accepts load until the coefficient of friction is exceeded. Once it is exceeded, the stiffness changes to a value that is nearly zero (Schrage 1981). The initial stiffness is calculated by equation given in Choi (2002). The shear modulus of elastomeric bearings is specified according to their hardness as per AASHTO (1996). Average value of shear modulus recommended range by AASHTO (1996) is assumed for this study. The dynamic coefficient of friction between the concrete surface and bearings, which is specified as 0.40 by Caltrans (2006) is employed in determining the ultimate shear capacity of bearing pad. The bilinear model for isolation bearing is shown in Fig. 3b along with bearing geometry (Fig. 3a).

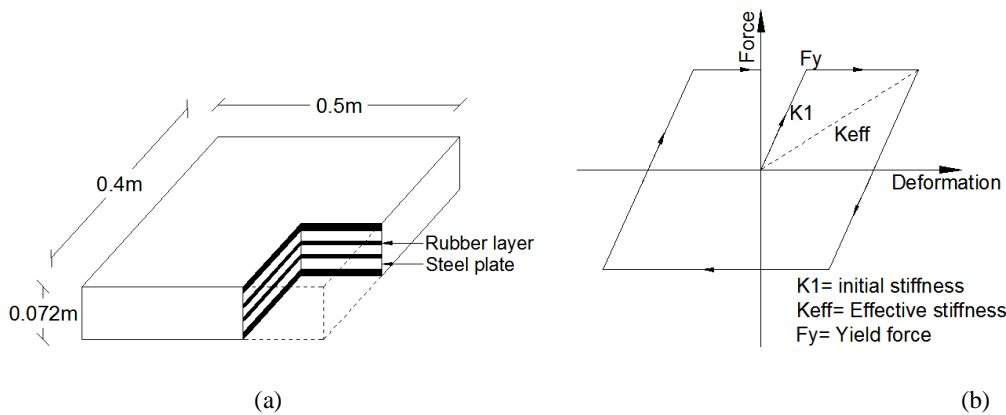


Figure 3. (a) Typical arrangement of isolation bearing (b) bilinear model of rubber bearing.

4 SEISMIC FRAGILITY FUNCTION

Fragility functions describe the conditional probability, i.e. the likelihood of a structure being damaged beyond a specific damage level for a given ground motion intensity (Billah & Alam 2014b). The fragility or conditional probability can be expressed as

$$\text{Fragility} = P[DS|IM = y] \quad (1)$$

where DS is the specified damage state of the structure or structural component at the given IM (the ground motion intensity measure) level and y is the realized condition of the ground motion intensity measure.

In this study, a probabilistic seismic demand model (PSDM) was developed using nonlinear time-history analyses of the bridge system. The PSDM establishes a correlation between the engineering demand parameters (EDP) and the ground intensity measures (IM). Two approaches are used to develop the PSDM: the scaling approach (Alam et al. 2012, Zhang & Huo 2009) and the cloud approach (Choi et al. 2004, Mackie & Stojadinović 2004, Nielson & DesRoches 2007a, b). In the current study, the cloud method was employed in evaluating the seismic fragility functions of the bridge piers and isolation bearing. Ductility of the bridge pier and horizontal deformation of the isolation bearing are considered as the EDPs, and the PGA is utilized as the intensity measure (IM) of each ground motion record. A regression analysis is carried out to obtain the mean and standard deviation for each limit state by assuming the power law function in the cloud approach, (Cornell et al. 2002), which gives a logarithmic correlation between median EDP and the selected IM as expressed below.

$$EDP = a (IM)^b \text{ or } \ln(EDP) = \ln(a) + b \ln(IM) \quad (2)$$

where a and b are coefficients which can be estimated from a regression analysis of the response data. It is assumed that the EDPs follow log-normal distributions (Gardoni et al. 2003). The Incremental Dynamic Analysis (IDA) was carried out to create sufficient data for the probabilistic seismic demand model (Billah et al. 2013).

IDA was carried out by scaling each ground motion to ten intervals and generating 200 data sets for use in the regression analysis. For carrying out the IDA, the ground motions were applied from a very low PGA to the maximum PGA of the respective ground motion. It was possible to generate sufficient damage data corresponding to different intensity levels (Billah et al. 2013). The dispersion of the demand, $\beta_{EDP|IM}$ can be estimated from Equation 3 (Baker and Cornell 2006).

$$\beta_{EDP|IM} = \sqrt{\frac{\sum_{i=1}^N (\ln(EDP) - \ln(aIM^b))^2}{N-2}} \quad (3)$$

where N= number of total simulation cases.

It is now possible to generate the fragilities using Equation 4 (Padgett 2007).

$$P[LS|IM] = \Phi\left[\frac{\ln(IM) - \ln(IM_n)}{\beta_{comp}}\right] \quad (4)$$

where $\Phi[]$ is the standard normal cumulative distribution function and

$$\ln(IM_n) = \frac{\ln(S_c) - \ln(a)}{b} \quad (5)$$

IM_n is defined as the median value of the intensity measure and $\ln(IM_n)$ is the natural log of the median IM value for the chosen damage state (slight, moderate, extensive, and collapse) discussed in next section, whereas a and b are the regression coefficients of the PSDMs and the dispersion component is presented in Equation 6 (Padgett 2007).

$$\beta_{comp} = \frac{\sqrt{\beta_{EDP|IM} + \beta_c^2}}{h} \quad (6)$$

where S_c is the median and β_c is the dispersion value for a particular damage state of the bridge pier.

The uncertainty associated with each of the limit states is characterized by assigning coefficients of variation (COV) to each damage state. Smaller values of COV are assumed for slight and moderate damage states ($COV_{slight} = COV_{moderate} = 0.25$) while larger values are adopted for the higher damage states ($COV_{extensive} = COV_{complete} = 0.5$). The logarithmic standard deviation or the dispersion is calculated using the following equation provided by Nielson (2005).

$$\beta_c = \sqrt{\ln(1 + COV^2)} \quad (7)$$

Fragility function of the bridge system is more convincing than the component level fragility function (Choi et al. 2004, Nielson & DesRoches 2007a,b, Zhang & Huo 2009). The first order reliability theory can be used to derive the upper and lower bounds on the system fragility function. Following the first order reliability theory and considering the series system, the global damage state of the system can be evaluated by considering the largest damage state at component level as follows.

$$DS_{system} = \max(DS_{pier}, DS_{bearing}) \quad (8)$$

The lower bound of the system fragility gives un-conservative estimate of the failure probability of the system, whereas the upper bound indicates the conservative estimate of the failure probability of the system which can be mathematically expressed as

$$\max_{i=1}^n [P(F_i)] \leq P(F_{system}) \leq 1 - \prod_{i=1}^n [1 - P(F_i)] \quad (9)$$

where $P(F_i)$ and $P(F_{system})$ is the likelihood of reaching the prescribed limit of damage state of the component and system, respectively.

5 CHARACTERIZATION OF DAMAGE STATES

For seismically isolated highway bridges, bridge piers and isolation bearings are the most critical components, which are often forced to enter into nonlinear range of deformations under strong earthquakes. Different forms of EDPs such as ductility of bridge piers and horizontal deformation of isolation bearings are used to measure the damage state (DS) of the bridge components. Four damage states as defined by HAZUS-MH (FEMA 2003) are commonly adopted in the seismic vulnerability assessment of engineering structures, namely slight, moderate, extensive and collapse damages. Table 3 summarizes the definitions of various damage states and

their corresponding damage criteria available in the literature. The damage states of isolation devices are determined based on experimental observation as well as consideration of resulting pounding and unseating. Typically either the bearing displacement or shear strain is used to describe the damage states (Alam et al. 2012, Bhuiyan & Alam 2012). Modern isolation bearings can experience shear strain up to 400% before failure, such large shear strain will result in large displacement and can cause significant pounding or unseating problem in the bridge system. Therefore, once the shear strain exceeds 250%, it is considered as complete damage of the bearing (JRA 2002).

Table 3. Damage state of bridge components.

Damage State	→	Slight (DS= 1)	Moderate (DS= 2)	Extensive (DS= 3)	Collapse (DS= 4)	Reference
Bridge components	Physical phenomenon	Cracking and spalling	Moderate cracking and spalling	Degradation without collapse	Failure leading to collapse	FEMA (2003)
Bridge pier	Displacement ductility μ_d	$\mu_d > 1.0$	$\mu_d > 1.2$	$\mu_d > 1.76$	$\mu_d > 4.76$	Hwang et al. (2001)
Isolation bearing	Shear strain γ (%)	$\gamma > 100$	$\gamma > 150$	$\gamma > 200$	$\gamma > 250$	Zhang and Huo (2009)

6 SEISMIC GROUND MOTION RECORDS

A suite of 20 earthquake ground motion records, which are assigned as medium to strong magnitude earthquake ground motions with PGA values ranging from 0.37g to 1.07g have been considered in the current study. The characteristics of the earthquake ground motion records are presented in Table 4. Figure 4a shows the acceleration response spectra with 5% damping ratio of the recorded ground motions. The mean amplitude of the earthquake records is also accompanied in the figure. Figure 4b shows the different percentiles of acceleration response spectra with 5% damping ratio illustrating that the selected earthquake ground motion records are well describing the medium to strong intensity earthquake motion histories.

Table 4. Characteristics of the earthquake ground motion histories.

Sl. No.	Earthquake	Year	Richter magnitude	PGA (g)
1	Tabas	1978	7.4	0.90
2	Tabas	1978	7.4	0.96
3	Loma Prieta	1989	7	0.70
4	Loma Prieta	1989	7	0.46
5	Loma Prieta	1989	7	0.67
6	Loma Prieta	1989	7	0.37
7	C. Mendocino	1992	7.1	0.63
8	C. Mendocino	1992	7.1	0.65
9	Erzincan	1992	6.7	0.42
10	Erzincan	1992	6.7	0.45
11	Landers	1992	7.3	0.69
12	Landers	1992	7.3	0.79
13	Nothridge	1994	6.7	0.87
14	Nothridge	1994	6.7	0.38
15	Nothridge	1994	6.7	0.72
16	Nothridge	1994	6.7	0.58
17	Kobe	1995	6.9	1.07
18	Kobe	1995	6.9	0.56
19	Kobe	1995	6.9	0.77
20	Kobe	1995	6.9	0.42

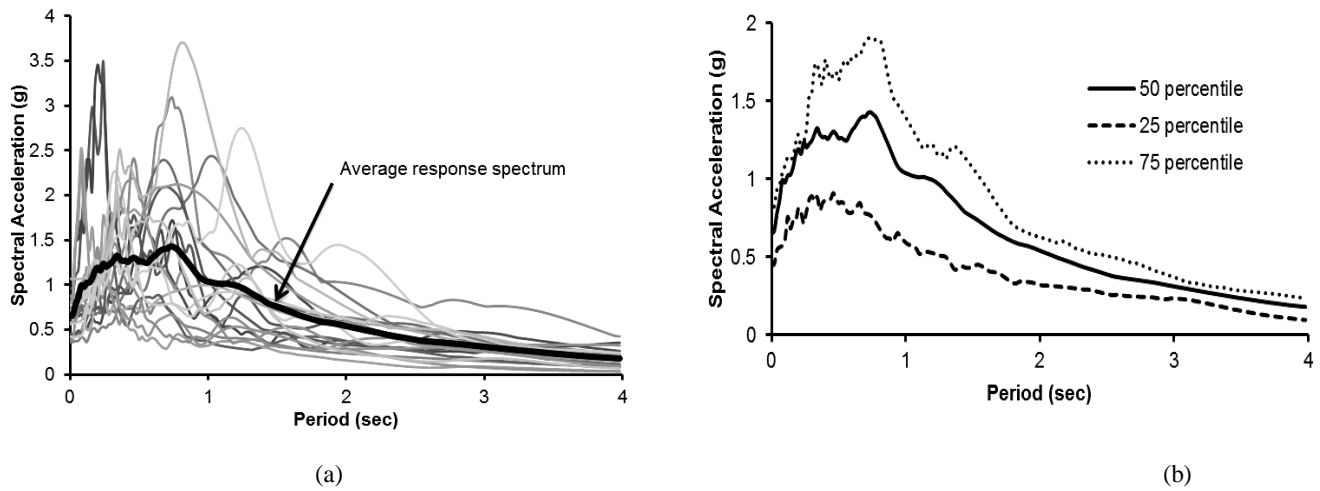


Figure 4. Earthquake ground motion records (a) response acceleration spectra, (b) percentiles of response acceleration spectra of a suit of 20 near field earthquake ground motion records. The values PGAs range from 0.37 to 1.07 g.

7 NUMERICAL RESULTS AND DISCUSSION

In order to assess the seismic vulnerability of a three-span highway bridge, seismic fragility curves for the piers and isolation bearings are generated using the numerical results obtained from the nonlinear incremental dynamic analysis. The PSDMs are developed by analyzing the limit placed on the bridge piers through a regression analysis. The PSDMs are constructed from the peak response of the bridge pier obtained from the IDA. Figure 5 shows the PSDMs for the bridge pier for ductility demand and isolation bearing piers for shear strain (%). Parameters a , b and β_{EDPIIM} are estimated from the regression analysis. The fragility can be directly estimated from the limit state capacity of each damage state as well as the PSDM parameters obtained from regression analysis. Utilizing these parameters, the fragility curves for the components are generated using equation 4. The fragility curves of a bridge system can be subsequently constructed by combining the fragility curves as obtained for each bridge component (pier and isolation bearing). Using the first order reliability theory (Eq. 8 and 9), the fragility curves for the bridge system are generated for each damage state.

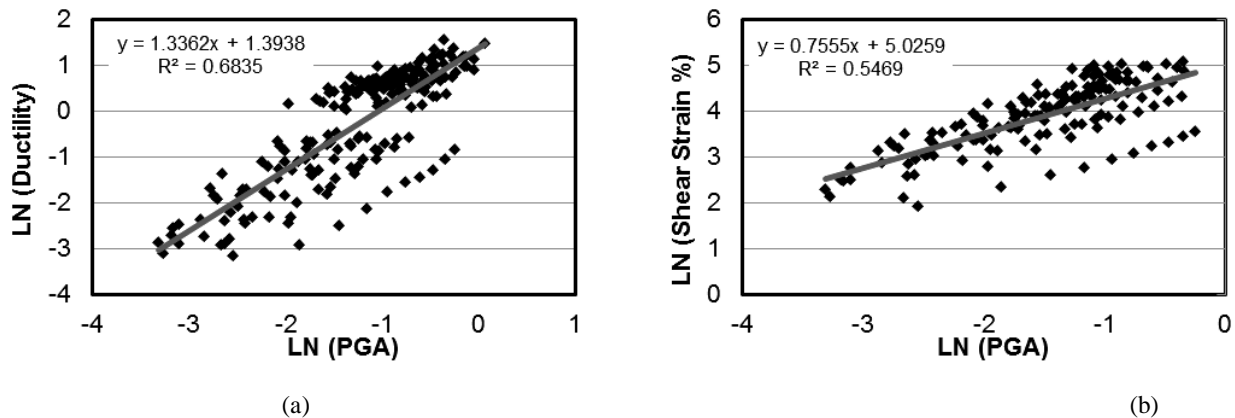


Figure 5. PSDMs for (a) bridge pier considering ductility demand, (b) isolation bearing considering shear strain (%).

The fragility curves of the bridge at component levels, i.e. bridge piers and isolation bearings are presented in Figure 6 and 7, respectively. The most vulnerable pier is considered in deriving the fragility curves for different damage states (DS) such as slight, medium, extensive and collapse as recommended by HAZUS-MH (FEMA 2003). As can be observed from Figure 6, seismic vulnerability of the bridge pier in slight, moderate and extensive damage states are much higher than collapse state indicating cracking and spalling probability in the pier (as shown in Table 3) even in low earthquake intensity level. On the contrary, fragility of isolation bearing shows less susceptibility to the applied ground motions (Fig. 7). A total of ten isolation bearings are used at the bridge pier segment and five at the abutment locations to accommodate the vertical and lateral deformations as experienced from the vertical compressive loadings of the bridge deck and the earthquake ground motions. Only the most vulnerable bearing is utilized to derive the fragility curves. Evidently, the damage probabilities of bearings are much lower than that of bridge piers.

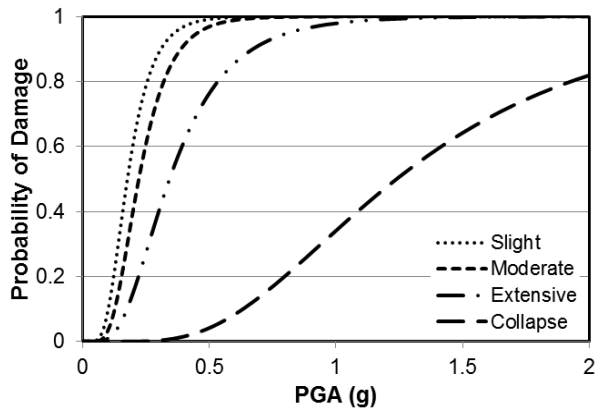


Figure 6. Fragility curves of the bridge pier.

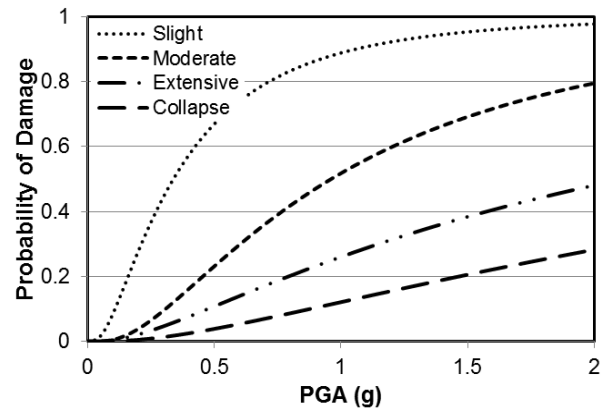


Figure 7. Fragility curves of isolation bearings.

Figure 8 represents the damage probability for the total bridge system. The four damage states are displayed to illustrate the seismic fragility of the bridge system. The figure indicates that the seismic fragility of the bridge system is largely dictated by the fragility of bridge piers over isolation bearing. Similar trends are also observed in the fragility curves at component levels (Fig. 6, 7).

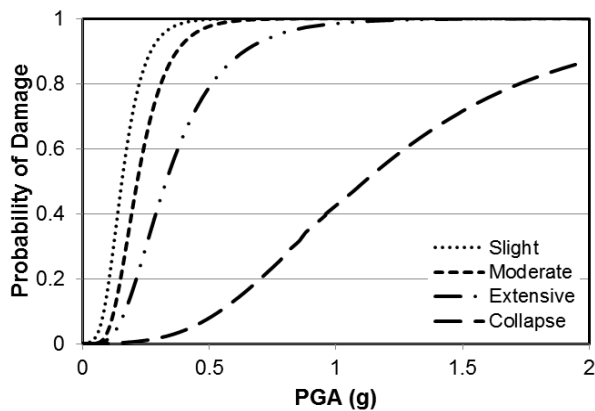


Figure 8. Fragility curves of the bridge system.

8 CONCLUDING REMARKS

Fragility assessment of a typical three-span continuous highway bridge in Bangladesh is conducted in this study through analytical simulation. The fragility curves are generated by analyzing the bridge both in the longitudinal and transverse direction. From IDA-based scaling approach using 20 near-field earthquake ground motion records, most vulnerable conditions are used to generate the data required for the formation of fragility curves. The numerical results show that the bridge piers are more susceptible to damage for the given medium to strong seismic ground motions as compared to those of the isolation bearings. These obtained curves can be potentially used to estimate the probable losses incurred from earthquakes, retrofitting prioritization and post-earthquake rehabilitation decision making.

REFERENCES

- AASHTO 1996. AASHTO Guide Specifications for LRFD Seismic Bridge Design, *American Association of State Highway and Transportation Officials 16th Ed. with 2001 Interims*, Washington D.C.
- Alam, M.S., Bhuiyan, A.R. & Billah, A.H.M.M. 2012. Seismic fragility assessment of SMA- bar restrained multi-span continuous highway bridge isolated with laminated rubber bearing in medium to strong seismic risk zones. *Bulletin of Earthquake Engineering*, 10(6): 1885-1909.
- Alam, M.S., Youssef, M.A. & Nehdi, M. 2008. Analytical prediction of the seismic behavior of superelastic shape memory alloy reinforced concrete elements. *Eng Struct*, 30(12):3399-3411.
- Applied Technology Council (ATC) 1985. *Earthquake damage evaluation data for California*. Report No. ATC-13.

- Baker, J.W. & Cornell, C.A. 2006. Vector-valued ground motion intensity measures for probabilistic seismic demand analysis. *Pacific Earthquake Engineering Research report 2006/08*, PEER Center, University of California Berkeley.
- Basöz, N., Kiremidjian, A.S., King, S.A. & Law, K.H. 1999. Statistical analysis of bridge damage data from the 1994 Northridge, CA, earthquake. *Earthq Spectra*, 15(1):25–54.
- Bhuiyan, M.A.R. & Alam, M.S. 2012. Seismic Vulnerability Assessment of a Multi-Span Continuous Highway Bridge Fitted with Shape Memory Alloy Bars and Laminated Rubber Bearings. *Earthquake Spectra*, 28(4): 1379-1404.
- Billah, A.H.M.M. & Alam, M.S. 2012. Seismic performance of concrete columns reinforced with hybrid shape memory alloy and fibre reinforced polymer bars. *Constr Build Mater*, 28(3):730–742.
- Billah, A.H.M.M. & Alam, M.S. 2014a. Seismic Fragility Assessment of Highway Bridges: A State-of-The-Art Review. In Press: *Structure and Infrastructure Engineering*, DOI:10.1080/15732479.2014.912243.
- Billah, A.H.M.M. & Alam, M.S. 2014b. Seismic fragility assessment of concrete bridge pier reinforced with superelastic Shape Memory Alloy. *Earthquake Spectra*, DOI: <http://dx.doi.org/10.1193/112512EQS337M>
- Billah, A.H.M.M., Alam, M.S. & Bhuiyan, A.R. 2013. Fragility analysis of retrofitted multi-column bridge bent subjected to near fault and far field ground motion. *ASCE Journal of Bridge Engineering*, 18(10):992-1004.
- Buckle, I.G. & Mayes, R.L. 1990. Seismic isolation: history, application, and performance- a world view. *Earthq Spectra*, 6:161–201.
- Caltrans 1990. Caltrans Structures Seismic Design References (first edition). *California Department of Transportation*, Sacramento, CA.
- Caltrans 2006. Seismic Design Criteria Version 1.4. *California Department of Transportation*, Sacramento, CA.
- Choi, E. 2002. Seismic Analysis and Retrofit of Mid-America Bridges. *PhD thesis*, Georgia Institute of Technology.
- Choi, E., DesRoches, R. & Nielson, B.G. 2004. Seismic fragility of typical bridges in moderate seismic zones. *Eng Struct*, 26:187–199.
- Cornell, A.C., Jalayer, F. & Hamburger, R.O. 2002. Probabilistic basis for 2000 SAC federal emergency management agency steel moment frame guidelines. *J. Struct. Eng.*, 128: 526–532.
- Dezfuli, F.H. & Alam, M.S. 2013. Shape memory alloy wire-based smart natural rubber bearing. *Smart Mater. Struct*, 22: 045013 (17pp).
- Federal Emergency Management Agency (FEMA) 2003. *HAZUS-MH software*, Washington DC
- Ferdousi, S. & Rahman, M.T. 2010. Earthquake in Bangladesh: How much are we prepared to face it? *Bangladesh J Pathol*, 25(1): 1-2.
- Gardoni, P., Mosalam, K.M. & Der Kiureghian, A., 2003. Probabilistic seismic demand models and fragility estimates for RC bridges. *J. Earthquake Eng.*, 7(1), 79–106.
- Ghobarah, A. & Ali, H.M. 1988. Seismic performance of highway bridges. *Eng Struct*, 10:157–166.
- Hwang, H., Jernigan, J.B. & Lin, Y.W. 2000. Evaluation of seismic damage to Memphis bridges and highway systems. *J Bridge Eng ASCE*, 5:322–330.
- Hwang, H., Liu, J.B. & Chiu, Y.H. 2001. Seismic fragility analysis of highway bridges. *MAEC report: project MAEC RR-4*. Mid-America Earthquake Center, Urbana.
- JRA 2002. Specifications for highway bridges-part V: seismic design. *Japan Road Association*, Tokyo, Japan
- Kelly, J.M. 1997. Earthquake resistant design with rubber (2nd edition). *Springer-Verlag Berlin Heidelberg*, New York
- Mackie, K.R. & Stojadinović, B. 2004. Fragility curves for reinforced concrete highway overpass bridges. *13th WCEE*, ID 1553
- Nielson, B.G. 2005. Analytical fragility curves for highway bridges in moderate seismic zones. *Ph.D. thesis*, Georgia Institute of Technology, Atlanta.
- Nielson, B.G. & DesRoches, R. 2007a. Seismic fragility curves for typical highway bridge classes in the central and southeastern United States. *Earthq Spectra*, 23:615–633.
- Nielson, B.G. & DesRoches, R. 2007b. Seismic fragility methodology for highway bridges using a component level approach. *Earthq Eng Struct Dyn*, 36:823–839.
- Novak, M. 1974. Dynamics stiffness and damping of piles. *Canadian Geotechnical Journal*, 11:574-598.
- Novak, M. & Howell, J. 1977. Torsional vibrations of pile foundations. *Journal of Geotechnical Engineering*, 103:271-285.
- Novak, M. & Sharnouby, B. E. 1983. Stiffness constants of single piles. *Journal of Geotechnical Engineering*, 109(7):961-974.
- Padgett, J.E. 2007. Seismic vulnerability assessment of retrofitted bridges using probabilistic methods. *PhD Thesis*, Georgia Institute of Technology, Atlanta.
- Poulos, H. G. 1971. Behavior of laterally loaded piles: I - pile groups. *American Society of Civil Engineering*, 97:733-751.
- Prakash, S. & Puri, V.K. 1988. Foundations for machines: analysis and design. *John Wiley and Sons*, New York.
- Prakash, S. & Sharma, H.D. 1990. Pile foundations in engineering practice. *John Wiley and Sons*, NY.
- Schrage, I. 1981. Anchoring of Bearings by Friction.” Joint Sealing and Bearing Systems for Concrete Structures. *World Congress on Joints and Bearings*, 1.
- SeismoStruct 2014. *SeismoStruct help file*. Available from www.seissoft.com
- Shinozuka, M., Feng, M.Q., Kim, H.K. & Kim, S.H. 2000. Nonlinear static procedure for fragility curve development. *J Eng Mech ASCE*, 126:1287–1295.
- Zhang, J. & Huo, Y. 2009. Evaluating effectiveness and optimum design of isolation devices for highway bridges using the fragility function method. *Eng Struct*, 31:1648–1660.